The Simulation Of Slat Noise Applying Stochastic Sound Sources Based On Solenoidal Digital Filters (SDF)

Roland Ewert[1]
roland.ewert@dlr.de

[1] DLR, Deutsches Zentrum für Luft- und Raumfahrt e.V.
Institut für Aerodynamik und Strömungstechnik, Technische Akustik
Lilienthalplatz 7, 38108 Braunschweig, Germany

Abstract

A new fast and cheap stochastic approach is introduced to model the unsteady turbulent sound sources in the slat-cove of a high-lift airfoil. It is based on the spatial filtering of a random white-noise field and incorporates information about the integral length scale and the turbulent kinetic energy from a steady RANS computation. The stochastic method, which is based on the LES inflow boundary condition proposed by Klein et al. [8] to reproduce first- and second-order one-point statistics, is extended in this paper for aeroacoustic applications. The extended formulation yields a solenoidal velocity field that is capable to reproduce exactly the complete second-order two-point correlation tensor of homogeneous isotropic turbulence. Results for the sound generation at the slat are given for the underlying RANS mean-flow field being based on a Menter SST turbulence model with Kato-Launder modification. The results for the modeled turbulent flow-field and the radiated acoustic field exhibit physical meaningful characteristics.

Keywords: CAA, APE, SDF, Slat Noise

1 Introduction

Aircraft noise reduction as achieved through the development and application of high bypass low noise turbofan engines has shifted the focus of interest to airframe noise as an equally important noise source during the approach phase. Experimental studies have identified deployed slats as prominent noise contributors [3, 10].

To reduce noise levels further, numerical tools will become necessary in the future to achieve an optimized low noise design of airframe components.

In the last years numerical techniques evolved in the framework of Computational Aeroacoustics (CAA) that are optimized for the simulation of wave propagation, i.e., high-order non-dispersive spatial and temporal discretization schemes and high-quality non-reflecting boundary conditions. A key point is how an acoustic solver based on the Euler perturbation equations or derivatives of it can be used for design-to-noise approaches to airframe components. A presumably accurate noise prediction methodology arises if appropriate acoustic sources of the propagation equations are computed from time accurate LES or DNS simulations of the turbulent near field. However, such approaches are too expensive to be considered for a design process that demands to evaluate design modification in short response times. In this paper a slat noise problem is studied using a cheaper computational approach that involves CAA techniques in conjunction with stochastic sound sources in the time domain.

2 Methods and Results

Acoustic perturbation equations (APE) [4, 5] are used to describe the evolution of small acoustic perturbations over a steady and viscous mean-flow. The mean-flow is determined from a steady RANS simulations applying a Menter SST turbulence model. As a major vortex source term the fluctuating Lamb vector $\vec{L}' = \vec{\omega} \times \vec{u} - \overline{\vec{\omega} \times \vec{u}}$ appears, where $\vec{\omega}$ and $\vec{u}$ denote the flow vorticity and velocity, respectively, and the overlined terms are time averaged.

A new technique is introduced to generate broadband stochastic sound sources in the time-domain, which is based on the digital filtering of random data. The method, originally proposed as a LES inflow boundary condition that accurately reproduces first- and second-order one-point statistics, is extended in this paper to prescribe a fully solenoidal velocity field on a predefined source patch in the interior CAA domain (Solenoidal Digital Filtering, SDF). The extended digital filtering procedure is the discrete realization of the continuous filtering integral

$$\psi(\boldsymbol{x}, t) = \int_{\boldsymbol{x}'} G\left[|\boldsymbol{x} - \boldsymbol{x}'|, \Delta(\boldsymbol{x}'), \hat{A}(\boldsymbol{x}')\right] \, \mathcal{U}(\boldsymbol{x}') d\boldsymbol{x}'. \tag{1}$$

In Eq. (1) G is the filter kernel, $\mathcal{U}$ denotes an unity white-noise field, and ψ is a fluctuating stream-function, which determines the pseudo-turbulent velocity fluctuations via

$$u_t' = \frac{\partial \psi}{\partial y}, \qquad v_t' = -\frac{\partial \psi}{\partial x}. \tag{2}$$

Hence, the approach yields strictly divergence-free or solenoidal velocity fluctuations. The filter kernel

$$G(r, \Delta, \hat{A}) = \hat{A} \exp\left(-\frac{\pi}{2}\frac{r^2}{\Delta^2}\right) \tag{3}$$

has two free parameters, i.e., the filter width Δ and the filter amplitude $\hat{A}$, which are determined from a steady RANS solution. Closer scrutinize reveals the constants to be

$$\Delta = \frac{c_l}{C_\mu}\frac{\overline{k}^{1/2}}{\omega} \approx 6.00\frac{\overline{k}^{1/2}}{\omega}, \qquad \hat{A} = \sqrt{\frac{2}{3\pi}}\overline{k}^{1/2} \approx 0.460\overline{k}^{1/2}. \tag{4}$$

More details can be found in [6]. The solenoidal extension can be shown to reproduce exactly the second-order two-point correlation tensor of homogeneous isotropic turbulence [1]

$$R_{ij}(r) = [f(r) - g(r)]\, n_i n_j + g(r)\delta_{ij}, \tag{5}$$

where δ_{ij} is the Kronecker symbol, and $r = \sqrt{\Delta x^2 + \Delta y^2}$ is the relative distance between two points '1' and '2'. The vector components n_i stand for the unity vector in the $\boldsymbol{r}_1 - \boldsymbol{r}_2$ direction. Fig. 1 shows a snapshot of the ω_3 vorticity component of the fluctuating pseudo-turbulent field. The mean-flow is uniform and running from left to right. From the corresponding fluctuating velocity field the tensor components of Eq. (5), $R_{ij} = \overline{u_i u_j}$, with $u_1 = u_t'$ and $u_2 = v_t'$, are processed. The normal vector components in Eq. (5) become $n_1 = \Delta x/r$, and $n_2 = \Delta y/r$. The Figs. 4-6 juxtapose the analytical solution to the stochastically generated result. Almost perfect agreement is obtained.

Fig. 2 depicts the correlations along a horizontal cut $\Delta y = 0$. The black lines indicate the target distributions for the longitudinal correlation function f, the 2D lateral correlation function g and the theoretical correlation of the vorticity $\omega_3 = \partial v/\partial x - \partial u/\partial y$. The colored triangles represent the respective solutions from the post-processing of the pseudo turbulence. Almost perfect quantitative agreement is achieved. Fig. 3 shows computational results also including a time-scale into the model. The plot shows the longitudinal correlations for various time separations Δt. The black dash-dotted lines indicate the target functions for the spatial and temporal correlations and the black solid lines

show the corresponding results from the stochastic realization. Very good agreement is achieved between the target functions and the results of the stochastic model.

The new stochastic method provides some advantage over the classical approach using inverse Fourier transform. It is time- and memory-efficient, strictly solenoidal, and can easily be applied to the the highly non-uniform mean-flow field in the slat-cove region using local results for the kinetic turbulent energy and the corresponding turbulent length scale from the RANS solution. Furthermore, it avoids the occurrence of shear decorrelations and resolves broadband spectra continuously. A further extension to non-homogeneous anisotropic solenoidal flows is possible with the transformation proposed by Smirnov et al. [11].

For the slat noise simulations a modified high-lift configuration with retracted flap is chosen in order to avoid additional sound sources. DLR's CAA code PIANO is used for the acoustic study. The code is block-structured and based on the DRP finite difference scheme. The CAA grid consists of 25 blocks with about 250k mesh points. It resolves the acoustic field in a $5c \times 5c$ box, where c denotes the main-element chord length. Based on a dimensional chord length $c = 0.4$m, the grid is sufficient to resolve frequencies up to 12kHz.

The RANS mean-flow field is computed with DLR's unstructured flow-solver TAU. The free flow Mach number, which is considered in this paper is $M = 0.10$. A Menter SST turbulence model [9] with Kato-Launder modification [7] is used. Fig. 7 depicts the distribution of turbulent kinetic energy in the slat-cove region. Fig. 8 depicts the integral length scale distribution in the slat-cove region. The radius of the black circles in Fig. 8 indicate the size of the length-scale Δ of Eq. (3).

Fig. 9 shows a snapshot of the v-velocity field, generated from the solenoidal digital filtering (SDF) procedure, utilizing the RANS solutions of $\overline{k}$ and the length scale from the Kato-Launder model. The used method has a memory overhead of about 20MB, compared to 700MB memory requirement for the baseline CAA solver without source model. The results of the pseudo-turbulent flow field exhibit physical meaningful details: from the slat hook the flow structures emerge, as one would expect it from growing instabilities in a shear layer.

Fig. 10 shows a snapshot of the unsteady acoustic pressure field that is generated by the SDF source model. The acoustic field roughly corresponds to that one would expect from a dipole source placed at the slat trailing edge with its axis normal to the slat chord.

Fig. 11 depicts a narrow band spectrum for a point $1.5c$ below the slat trailing edge. The spectrum is related to a dimensional frequency, which corresponds to a model with 0.4m dimensional chord length. The visible narrow band decay is confined to a range between f^{-2} and f^{-3}, which roughly corresponds to the 12th octave decay between f^{-1} and f^{-2} that was found by Choudhari et al. [2] in measurements.

References

[1] Batchelor, G., *The Theory of Homogeneous Turbulence*, Cambridge University Press, 1960.

[2] Choudhari, M., Khorrami, M., Lockard, D., and Atkins, H., Slat Cove Noise Modeling: A Posteriori Analysis of Unsteady RANS Simulations, *AIAA Pap. 2002-2468*, 2002.

[3] Dobrzynski, W. and Pott-Pollenske, M., Slat Noise Studies for Farfield Noise Prediction, *AIAA Pap. 2001-2158*, 2001.

[4] Ewert, R. and Schröder, W., Acoustic Perturbation Equations Based on Flow Decomposition via Source Filtering, *J. Comp. Phys.*, vol. 188, pp. 365–398, 2003.

[5] Ewert, R. and Schröder, W., On the simulation of trailing edge noise with a hybrid LES/APE method, *Journal of Sound and Vibration*, vol. 270, pp. 509–524, 2004.

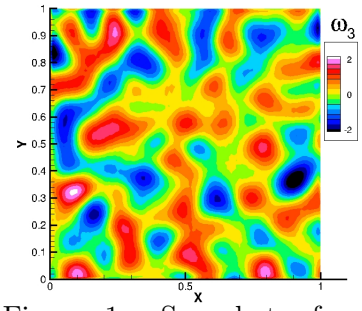

Figure 1: Snapshot of ω_3-vorticity.

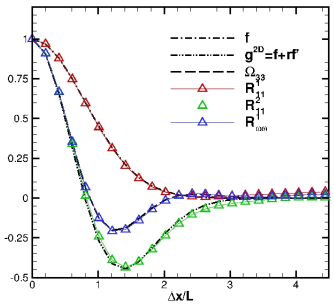

Figure 2: Spatial two-point correlations; black line: target function, colored triangles: reconstruction.

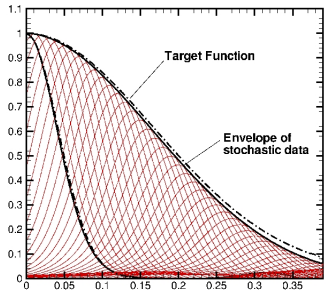

Figure 3: Two-point space-time correlations over separation distance Δx for different time differences Δt.

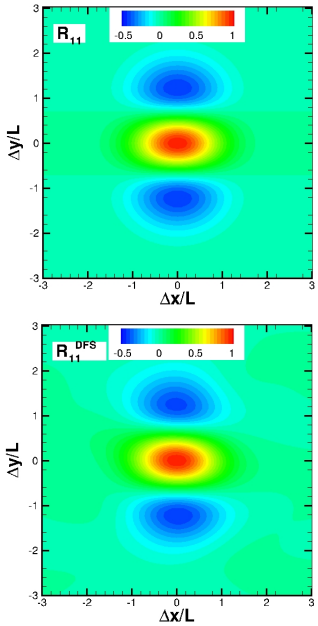

Figure 4: $R_{11}(\Delta x, \Delta y)$, top: analytical solution, bottom: stochastic realization.

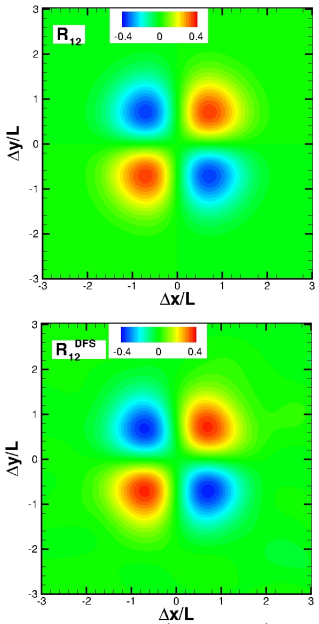

Figure 5: $R_{12}(\Delta x, \Delta y)$, top: analytical solution, bottom: stochastic realization.

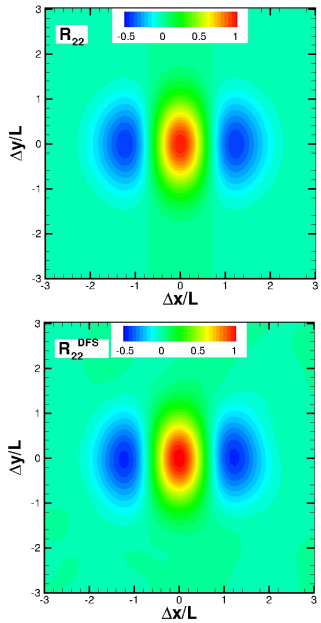

Figure 6: $R_{22}(\Delta x, \Delta y)$, top: analytical solution, bottom: stochastic realization.

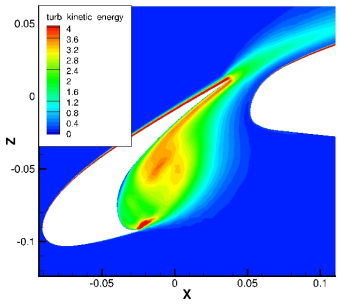

Figure 7: Turbulent kinetic energy in the slat-cove, $M = 0.10$.

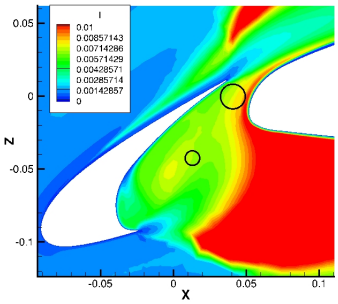

Figure 8: Length scale in the slat-cove, $c_l/C_\mu = 6.0$.

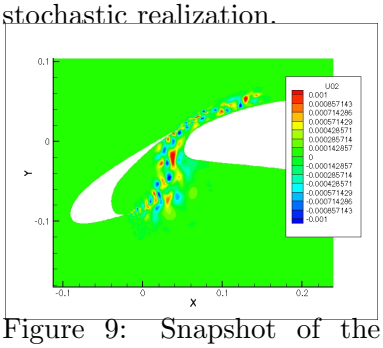

Figure 9: Snapshot of the v-component of the generated stochastic field, Kato-Launder.

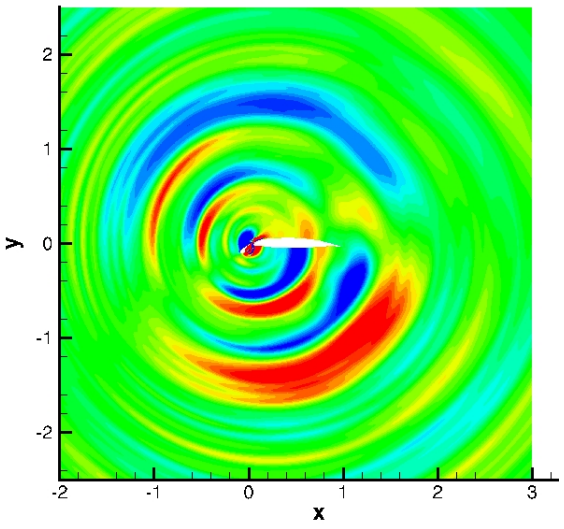

Figure 10: Sound pressure field.

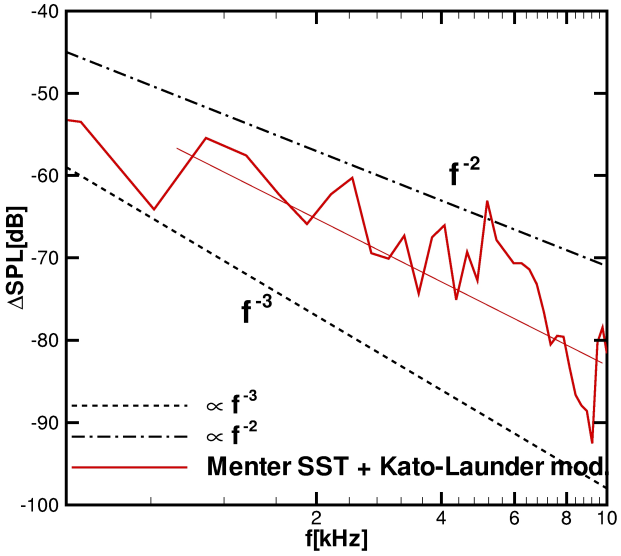

Figure 11: Narrow band spectra.

[6] Ewert, R., CAA Slat Noise Studies Applying Stochastic Sound Sources Based On Solenoidal Digital Filters, *AIAA Pap. 2005-2862*, 2005.

[7] Kato, M. and Launder, B., The modelling of turbulent flow around stationary and vibrating square cylinders, *9th symposium on turbulent shear flows, Kyoto, Japan, August 16th-18th, 1993*, 1993.

[8] Klein, M., Sadiki, A., and Janicka, J., A digital filter based generation of inflow data for spatially developing direct numerical or large eddy simulations, *J. Comp. Phys.*, vol. 186, pp. 652–665, 2003.

[9] Menter, F., Zonal Two Equation k-ω Turbulence Models for Aerodynamic Flows, *AIAA Pap. 93-2906*, 1993.

[10] Singer, B., Lockard, D., and Brentner, K., Computational Aeroacoustics Analysis of Slat Trailing-Edge Flow, *AIAA Journal*, Vol. 38(9), 2000.

[11] Smirnov, A., Shi, S., and Celik, I., Random Flow Generation Technique for Large Eddy Simulations and Particle Dynamics Modeling, *Journal of Fluids Engineering*, vol. 123, pp. 359–371, 2001.